Cell Research (2012) 22:1285-1303.

www.nature.com/cr

ORIGINAL ARTICLE

N-methylpurine DNA glycosylase inhibits p53-mediated cell cycle arrest and coordinates with p53 to determine sensitivity to alkylating agents

Shanshan Song[1, 2, 3], Guichun Xing[2, 3], Lin Yuan[2, 3], Jian Wang[2, 3], Shan Wang[2, 3], Yuxin Yin[4], Chunyan Tian[2, 3], Fuchu He[1, 2, 3], Lingqiang Zhang[2, 3]

[1]Department of Medical Genetics, Institute of Basic Medical Sciences, Chinese Academy of Medical Sciences & Peking Union Medical College, Beijing 100005, China; [2]State Key Laboratory of Proteomics, Beijing Proteome Research Center, Beijing Institute of Radiation Medicine, Beijing 100850, China; [3]National Engineering Research Center for Protein Drugs, Beijing 100850, China; [4]Department of Pathology, School of Basic Medical Sciences, Peking University, Beijing 100191, China

Alkylating agents induce genome-wide base damage, which is repaired mainly by *N*-methylpurine DNA glycosylase (MPG). An elevated expression of MPG in certain types of tumor cells confers higher sensitivity to alkylation agents because MPG-induced apurinic/apyrimidic (AP) sites trigger more strand breaks. However, the determinant of drug sensitivity or insensitivity still remains unclear. Here, we report that the p53 status coordinates with MPG to play a pivotal role in such process. MPG expression is positive in breast, lung and colon cancers (38.7%, 43.4% and 25.3%, respectively) but negative in all adjacent normal tissues. MPG directly binds to the tumor suppressor p53 and represses p53 activity in unstressed cells. The overexpression of MPG reduced, whereas depletion of MPG increased, the expression levels of pro-arrest gene downstream of p53 including p21, 14-3-3σ and Gadd45 but not pro-apoptotic ones. The N-terminal region of MPG was specifically required for the interaction with the DNA binding domain of p53. Upon DNA alkylation stress, in p53 wild-type tumor cells, p53 dissociated from MPG and induced cell growth arrest. Then, AP sites were repaired efficiently, which led to insensitivity to alkylating agents. By contrast, in p53-mutated cells, the AP sites were repaired with low efficacy. To our knowledge, this is the first direct evidence to show that a DNA repair enzyme functions as a selective regulator of p53, and these findings provide new insights into the functional linkage between MPG and p53 in cancer therapy.

***Keywords*:** MPG; p53; cell cycle arrest; base excision repair; alkylating agents

Cell Research (2012) **22**:1285-1303. doi:10.1038/cr.2012.107; published online 17 July 2012

Introduction

Living cells continually suffer damage as a consequence of normal cellular metabolism and as a result of attacks by environmental agents. Thus, the cell is continually faced with an agonizing choice: repair and live or die. Defects in this decision process can lead to cancer. The tumor suppressor p53 acts as a "traffic cop" to decide cell fate [1]. It is widely accepted that p53 is a sequence-specific transcription factor and plays a pivotal role in the regulation of cell cycle progression, apoptosis and DNA repair in response to diverse stress signals [2, 3]. In unstressed conditions, p53 is kept at an extremely low level due to rapid proteasomal degradation. However, under stress conditions p53 is stabilized and released from suppression [4].

There are at least two ways in which p53 is activated: posttranslational modifications and interactions with various proteins. A few proteins have been identified that associate with p53 to selectively regulate the expression of p53 downstream targets. For example, we recently found that ATM- and p53-associated KNZF protein (Apak), a KRAB-type zinc finger protein, interacts with p53 directly and specifically inhibits p53-mediated

Correspondence: Fuchu He[a]; Lingqiang Zhang[b]
[a]E-mail: hefc@nic.bmi.ac.cn
[b]E-mail: zhanglq@nic.bmi.ac.cn
Received 30 August 2011; revised 23 November 2011; accepted 1 February 2012; published online 17 July 2012

apoptosis [5]. Similarly, ASPP1/2 and hCAS have been shown to interact with p53 and specifically enhance p53-induced apoptosis but not cell cycle arrest [6, 7]. In contrast, Hzf binds to p53, and preferentially transactivates the pro-arrest p53 target genes [8]. Notably, Hzf itself is a downstream target gene of p53. When DNA damage occurs, Hzf is upregulated and then coordinates with p53 to induce the expression of cell cycle arrest genes [8]. In unstressed conditions, the regulation of p53-mediated cell cycle arrest, particularly the negative regulation, is still not fully understood.

To search for novel regulators of p53, we used high-density protein microarrays, as described previously [9]. Among the novel potential p53-interacting proteins, we found that *N*-methylpurine DNA glycosylase (MPG, also called AAG or ANPG), the first identified enzyme in the base excision repair (BER) pathway [10], can bind to p53 and selectively inhibit p53-mediated cell cycle arrest in cancer cells under normal physiological situations.

BER is the major DNA-repair process responsible for handling the DNA damage that is induced by exogenous and endogenous alkylating and oxidative agents and by spontaneous depurinations. As a core enzyme in BER, MPG has been shown to recognize and excise a broad range of modified bases, in addition to normal bases, in DNA. The removal of bases leaves repair intermediates, abasic (apurinic/apyrimidic, AP) sites, that are cytotoxic and mutagenic, which makes it apparent that the removal of these BER intermediates is crucial [11, 12]. Under certain conditions, an elevated expression of MPG was found to contribute to the formation of sister chromatid exchanges, chromosomal aberrations, frameshift mutagenesis and microsatellite instability [13-15]. Previous analysis showed that MPG expression was increased in certain human cancers including breast cancer cells. Ulcerative colitis (UC), a chronic inflammatory disease associated with an increased risk of developing colorectal cancer [16], was also observed to be associated with an increased level and activity of MPG [17].

Alkylating agents have been frequently used in the treatment of human cancers. Cancer cells can become resistant to the treatments, and high-dose chemotherapy may induce secondary cancers. The major DNA damage produced by alkylating agents is recognized and repaired by MPG; therefore, it is a good candidate molecular target for individualized therapy. It has been reported that reducing the levels of MPG protein using siRNA increased the sensitivity of cervical carcinoma cell lines to Temozolomide (TMZ), methyl methanesulfonate (MMS), *N*-methyl-*N*-nitrosourea (MNNG) and 1,3-bis(2-chloroethyl)-1-nitrosourea (BCNU) [18]. Reciprocally, overexpression of MPG was also deleterious to cells because more alkylating agent-induced AP sites and single- or double-stranded DNA breaks were produced [11, 12]. Collectively the above data suggest that an important role for MPG in carcinogenesis and that cancer therapy depends on its glycosylase activity to produce AP sites. Moreover, the varied responses of different cell types suggest that there are other molecules participating in the cellular response.

The crystal structure of the MPG-DNA complex shows that Tyr162 of the enzyme is intercalated into the space vacated by the lesion via the DNA minor groove, which helps maintaining proper base stacking and minimizing DNA distortion. Glu125 acts as a general base, deprotonating a water molecule in the nucleophilic attack on the N-glycosylic bond by an acid-base catalytic mechanism [19, 20]. To date, the function of the N-terminal part of MPG (aa 1-80) remains unclear.

Our current findings show that the MPG N-terminus is both sufficient and necessary for p53 binding and regulation. MPG specifically inhibits p53-mediated cell cycle arrest but not apoptosis. In response to alkylation damage, in p53 wild-type tumor cells, MPG dissociated from p53, resulting in the release of p53 and cell cycle arrest to allow for the repair of damaged bases. Thus, the combination of high levels of MPG with wild-type p53 in certain tumor cells led to insensitivity to alkylating agents. By contrast, in p53-mutated cells, the AP sites were repaired with low efficacy and the killing effects were higher than in the p53 wild-type cells. Therefore, MPG coordinates its glycosylase and non-glycosylase modules to participate in the DNA damage repair. Also, the p53 status coordinates with MPG to play a pivotal role in the determination of cancer sensitivity to alkylating drugs. To our knowledge, this is the first direct evidence to show that a DNA repair enzyme functions as a selective regulator of p53, and these findings provide new insights into the functional linkage between MPG and p53 in cancer therapy.

Results

MPG interacts with p53 in vitro and in vivo

To find new modulators of p53, we used a ProtoArray® Human Protein Microarray spotted with 8000 GST-tagged human proteins from multiple gene families on high-density glass slides (Invitrogen). All proteins were purified under nondenaturing conditions and printed at 4 °C to preserve their native structures and functions. Protein arrays (n = 3 per experimental group) were incubated with recombinant active p53 or assay buffer only. Software analysis was performed to evaluate the significant differences in the signal intensity between

control arrays and the arrays incubated with p53. A total of 28 potential p53-interacting proteins were identified, including casein kinase 1 and aurora kinase A, the known p53-binding proteins (Table 1). Among the previously unidentified potential p53-interactors is MPG, which has been demonstrated to be involved in the BER pathway and was further investigated in this study.

As the above assay represents an *in vitro* binding method, we next tested whether MPG interacts with p53 in cultured mammalian cells. Myc-tagged MPG and Flag-tagged p53 were expressed individually or together in p53-null H1299 cells followed by co-immunoprecipitation (Co-IP) assays. Indeed, MPG was co-immunoprecipitated with ectopic p53 (Figure 1A). Reciprocal assays showed that p53 was also co-immunoprecipitated with the ectopic MPG protein (Figure 1B). For negative controls, there was no p53 or MPG detected in anti-Myc or anti-Flag antibody immunoprecipitates from cells transfected with Myc-MPG or Flag-p53 alone, respectively (Figure 1A and 1B). To further confirm the interaction between MPG and p53, an *in vitro* GST pull-down assay was performed. As shown, GST-fused MPG, but not GST alone, could pull down Myc-p53 that was overexpressed in H1299 cells (Figure 1C). Similarly, GST-p53 could also pull down the Myc-MPG protein expressed in H1299 (Figure 1D). Importantly, endogenous MPG was easily co-immunoprecipitated with endogenous p53, but not by a control IgG in wild-type p53-expressing MCF7 breast cancer cells (Figure 1E) and in HEK293 human embryonic kidney cells (Supplementary information,

Table 1 The list of p53 binding proteins identified by protein microarray analysis

No.	Database ID	Protein Name
1	NM_005030.3	Homo sapiens polo-like kinase 1 (*Drosophila*) (PLK1)
2	NM_019095.3	Homo sapiens cardiolipin synthase 1 (CRLS1)
3	NM_001810	Homo sapiens centromere protein B, 80kDa (CENPB)
4	NM_005325.3	Homo sapiens histone cluster 1, H1a (HIST1H1A)
5	NM_004441.3	Homo sapiens EPH receptor B1 (EPHB1)
6	NM_032017.1	Homo sapiens serine/threonine kinase 40 (STK40)
7	BC001280.1	Homo sapiens aurora kinase A
8	NM_152376.2	Homo sapiens UBX domain containing 3 (UBXD3)
9	NM_032350.3	Homo sapiens hypothetical protein MGC11257 (MGC11257)/C7orf50
10	BC033088.1	Homo sapiens lamin A/C
11	BC006423.1	Homo sapiens aurora kinase A
12	NM_020631.2	Homo sapiens pleckstrin homology domain containing, family G (with RhoGef domain) member 5 (PLEKHG5), transcript variant 1
13	NM_001894.4	Homo sapiens casein kinase 1, epsilon (CSNK1E), transcript variant 2
14	NM_002497.2	Homo sapiens NIMA (never in mitosis gene a)-related kinase 2 (NEK2)
15	NM_053006.3	Homo sapiens testis-specific serine kinase 2 (TSSK2)
16	BC014991.1	Homo sapiens N-methylpurine-DNA glycosylase(MPG)
17	BC031691.2	Homo sapiens SLAIN motif family, member 2 (KIAA1458)
18	NM_017900.1	Homo sapiens aurora kinase A (AURKA), transcript variant 2
19	NM_001004023.1	Homo sapiens dual-specificity tyrosine-(Y)-phosphorylation regulated kinase 3 (DYRK3)
20	BC012109.1	Homo sapiens homer homolog 2 (*Drosophila*)
21	L18974.1	Homo sapiens megakaryocyte-associated tyrosine kinase (MATK)
22	NM_001039468.1	Homo sapiens MAP/microtubule affinity-regulating kinase 2 (MARK2)
23	NM_005105.2	Homo sapiens RNA binding motif protein 8A (RBM8A)
24	NM_138565.1	Homo sapiens cortactin (CTTN), transcript variant 2
25	NM_001031812.2	Homo sapiens casein kinase 1, gamma 3 (CSNK1G3)
26	NM_175887.2	Homo sapiens proline rich 15 (PRR15)
27	NM_001892.4	Homo sapiens casein kinase 1, alpha 1 (CSNK1A1)
28	NM_203454.1	Homo sapiens apolipoprotein B mRNA editing enzyme, catalytic polypeptide-like 4 (putative) (APOBEC4)

Seven protein interactions with p53 have been identified previously and therefore represent known interactions.

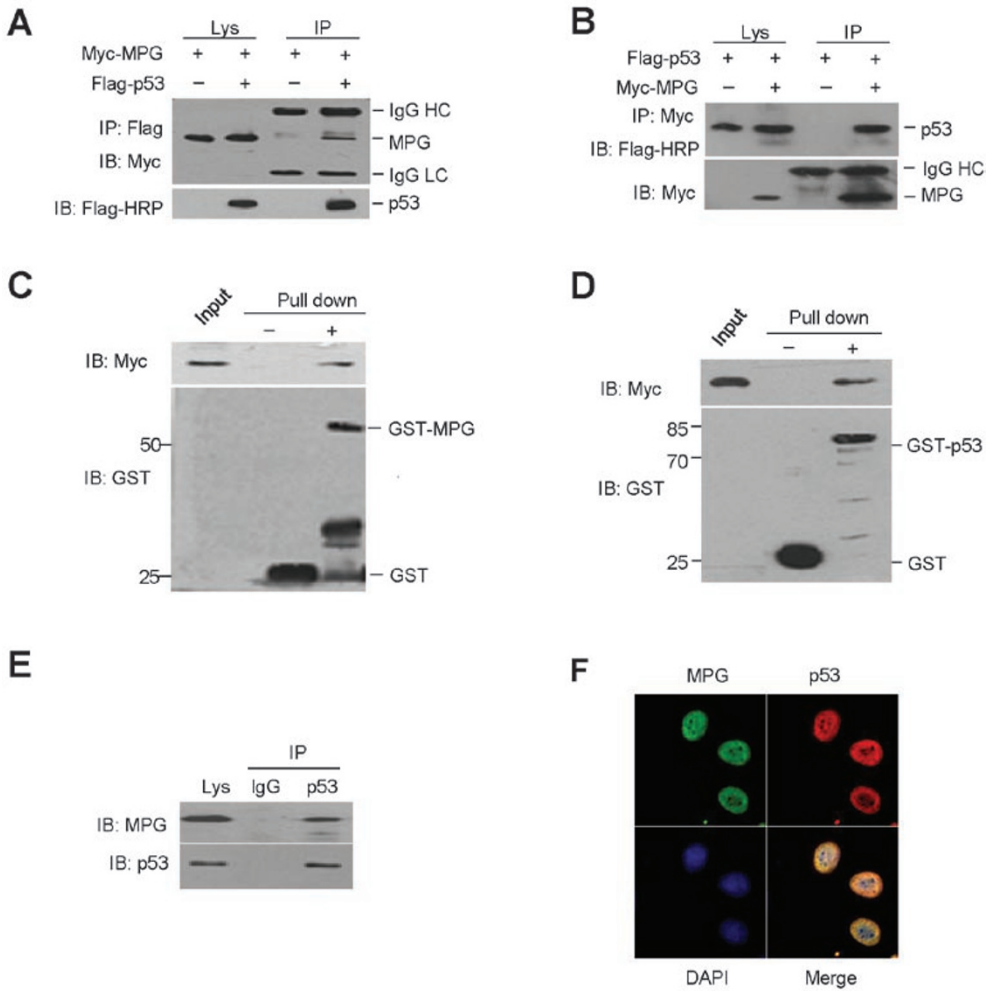

Figure 1 MPG interacts with p53. **(A**, **B)** Co-immunoprecipitation of exogenous MPG and p53 in H1299 cells. p53-null H1299 cells were transfected with Myc-tagged MPG and Flag-tagged p53. After 48 h, cell lysates were immunoprecipitated with anti-Flag or anti-Myc antibodies. The cell lysates and immunoprecipitates were detected by western blot analysis with anti-Myc or anti-Flag HRP antibodies, as indicated. **(C**, **D)** A direct interaction between MPG and p53 is shown by GST pull-down assays. The input and pull-down samples were analyzed with anti-GST and anti-Myc antibodies. Input represents 10% of the amount used for pull-down. **(E)** Co-immunoprecipitation of endogenous MPG and p53 in MCF7 cells. Whole-cell lysates were immunoprecipitated with p53 antibody (DO-1) or control IgG and analyzed by immunoblotting using p53 or MPG antibodies. Use of p53-HRP was only to detect the native protein. **(F)** The colocalization of MPG and p53 in the MCF7 cells. Indirect immunofluorescence analysis was performed. The cells were visualized by confocal microscopy, and the nuclei were stained with DAPI. IP, immunoprecipitation; IB, immunoblotting; Lys, lysate; IgG HC, heavy chain. IgG LC, light chain.

Figure S1A). Indirect immunofluorescence assays revealed that MPG and p53 were colocalized predominantly in the nucleoplasm of MCF7 cells (Figure 1F). These results indicate that p53 binds to MPG both *in vitro* and in cultured cells.

Determination of the mutual interaction regions in p53 and MPG

To reveal the molecular mechanism for the interaction of MPG and p53, we used various p53 and MPG deletion mutants to map the domains required for their interaction. As a well-defined transcription factor, p53 consists of an N-terminal transcriptional activation domain (TAD), a central DNA-binding domain (DBD) and a C-terminal regulatory domain (including an oligomerization domain and a basic domain) (Figure 2A). Co-immunoprecipitation assays showed that deletion of the N-terminal TAD domain of p53 (ND2, aa 113-393) or the C-terminal regulatory domain of p53 (CD1, aa 1-290) had no effects on the interaction between p53 and MPG (Figure 2B,

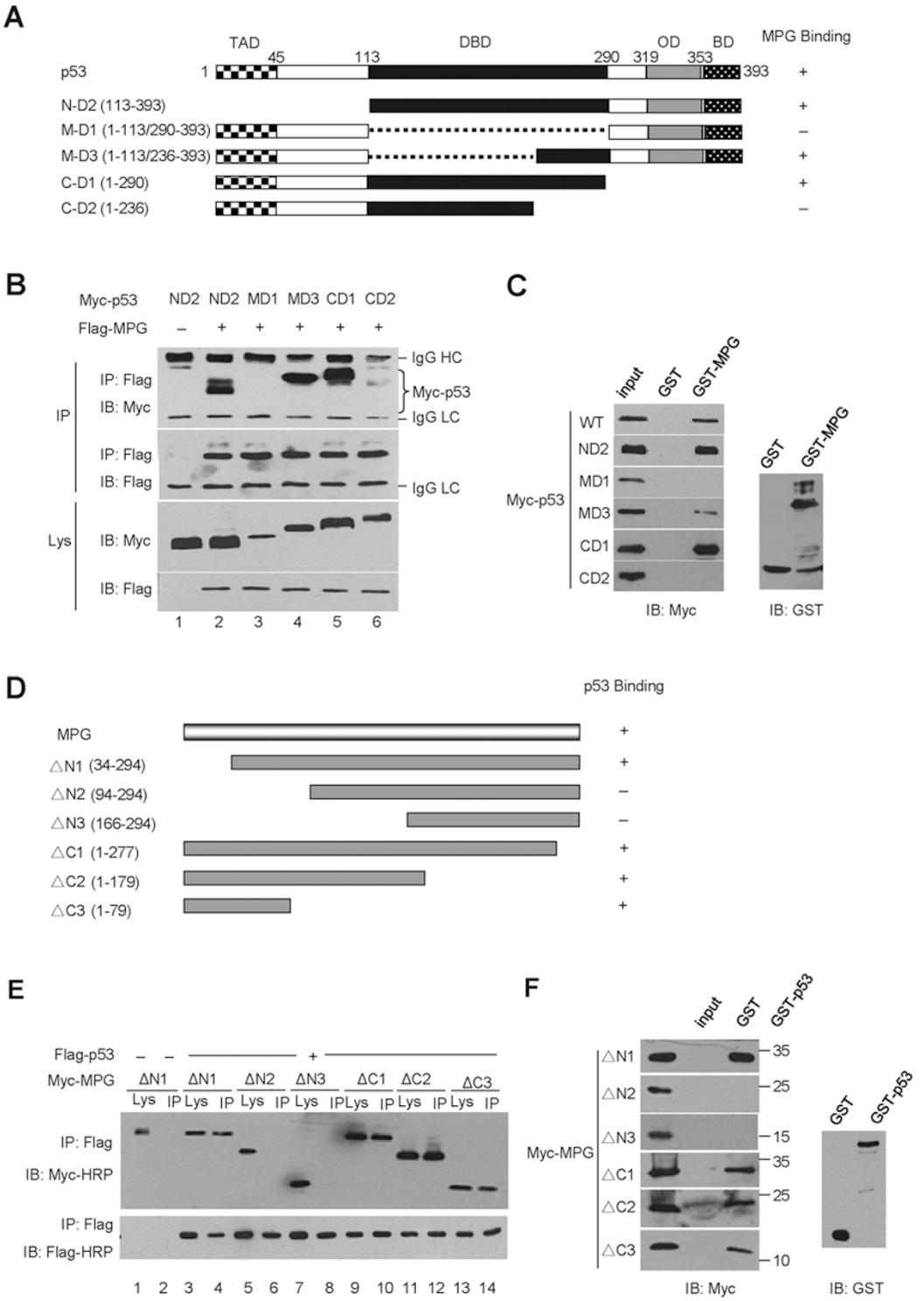

Figure 2 Determination of mutual interaction regions in p53 and MPG. **(A)** A diagram for the deletion mutants of p53 is shown. **(B)** Cell lysates from H1299 cells transfected with Flag-tagged MPG and Myc-tagged deletion mutants of p53 were immunoprecipitated with an anti-Flag antibody, followed by western blot analysis. **(C)** A GST pull-down assay for Myc-p53 truncations and GST or GST-MPG. Input and pull-down samples were analyzed with anti-GST and anti-Myc antibodies. Input represents 10% of the amount used for pull-down. **(D)** A diagram for the deletion mutants of MPG is shown. **(E)** Cell lysates from H1299 cells transfected with Flag-tagged p53 and Myc-tagged deletion mutants of MPG were immunoprecipitated with an anti-Flag antibody, followed by western blot analysis. **(F)** GST pull-down assay for Myc-MPG truncations and GST or GST-p53, as indicated.

lanes 1, 2 and 5). By contrast, deletion of the p53 central DBD (MD1, aa 1-113/290-393) abolished the binding (Figure 2B, lane 3). Furthermore, a careful examination of the DBD showed that the C-terminal part of the DBD (aa 237-290) was critical for the interaction (Figure 2B, lanes 4 and 6).

To confirm this result, we performed an *in vitro* GST pull-down assay. GST-fused MPG, but not GST alone, could pull down the ND2, MD3 and CD1 mutants of p53 and wild-type p53 but not the MD1 and CD2 mutants overexpressed in H1299 cells (Figure 2C). These results indicate that the region around aa 237-290 within the p53 DNA binding domain is critical for the MPG interaction.

Similarly, a series of MPG deletion mutants was generated (Figure 2D) and tested for the interaction with p53 through Co-IP (Figure 2E) and GST pull-down assays (Figure 2F). As shown, all of the examined MPG mutants, with the exception of ΔN2 (aa 94-294) and ΔN3 (aa 166-294), interacted with p53 in both assays (Figure 2E and 2F). These results suggest that the N-terminal aa 34-79 region of MPG is both sufficient and necessary for p53 binding.

Certain residues within the DNA binding domain of p53 play a key role in the MPG-p53 interaction

Given the fact that MPG binds to the DNA binding domain of p53, which represents the hot mutation region in human tumors, we next explored whether tumor-derived p53 mutations in the DBD had any effect on the interaction between MPG and p53. A total of six frequently observed mutations of this region, including R248Q, R273C, R273H, A266E, R280K and E285K, were examined. It has been reported that all of these mutants have either low or no transactivation function compared with wild-type p53 [21, 22]. The generated p53 mutants were first confirmed for their transcriptional activity through a pG13L luciferase reporter assay. As expected, all mutants had low (e.g., A266E and E285K) or almost no transcriptional activity (especially R248Q, R273C, R273H and R280K) on the pG13L reporter compared with wild-type p53 (Figure 3A), consistent with previous reports [23]. These mutants were then tested for the interaction with MPG through Co-IP assays. Strikingly, three of the four loss-of-function mutants (i.e., R248Q, R273C and R280K) dramatically lost the ability to interact with MPG (Figure 3B, lanes 3, 5 and 7). By contrast, the A266E and E285K mutants possessed a comparable MPG-binding ability with wild-type p53 (lanes 4 and 8). Reduced but still significant binding occurred with the R273H mutant for an unknown reason (lane 6). The re-

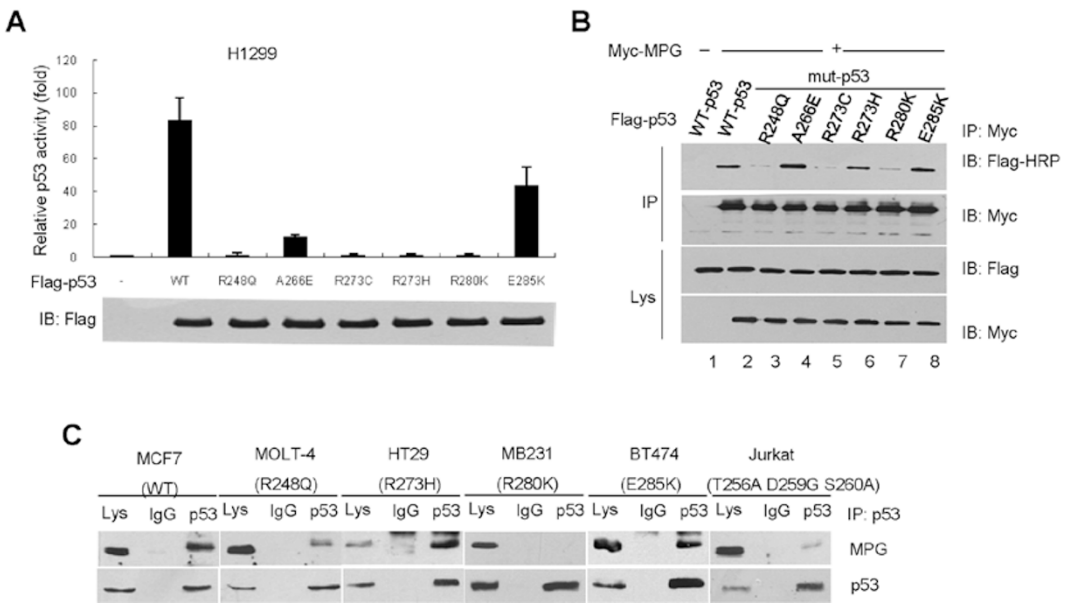

Figure 3 The effects of mutations in the DBD of p53 on the MPG-p53 interaction. **(A)** An analysis of the residual p53 transactivity of point mutations in H1299 p53-null cells. H1299 cells were co-transfected with the pG13-Luc reporter gene and with p53 point mutations. After 24 h, the luciferase assay was performed. Graph shows the mean ± SD of three independent experiments. SD, standard deviation. **(B)** Co-IP of p53 point mutants and MPG in H1299 cells. The indicated wild-type p53 or mutants were co-transfected with Myc-MPG or Myc vector. Cell lysates were immunoprecipitated with an anti-Myc antibody, followed by immunoblotting with anti-Flag-HRP and anti-Myc antibodies. **(C)** Co-IP of endogenous MPG and p53 in different p53 mutation cell lines as indicated.

sults indicate that R248, R273 and R280 of p53 are key residues for the interaction with MPG.

To further verify these results, we selected several tumor cell lines possessing the above p53 mutations to examine the possible endogenous MPG-p53 interaction, including leukemia MOLT4 (R248Q), human colon cancer (CC) HT29 (R273H), human breast cancer MDA-MB-231 (R280K), human breast cancer BT474 (E285K) and leukemia Jurkat (T256K, D259G, S260A) cell lines. Co-IP assays showed that endogenous R248Q (MOLT-4) and R280K (MB-231) had very weak interaction with MPG, whereas R273H (HT29) and E285K (BT474) had

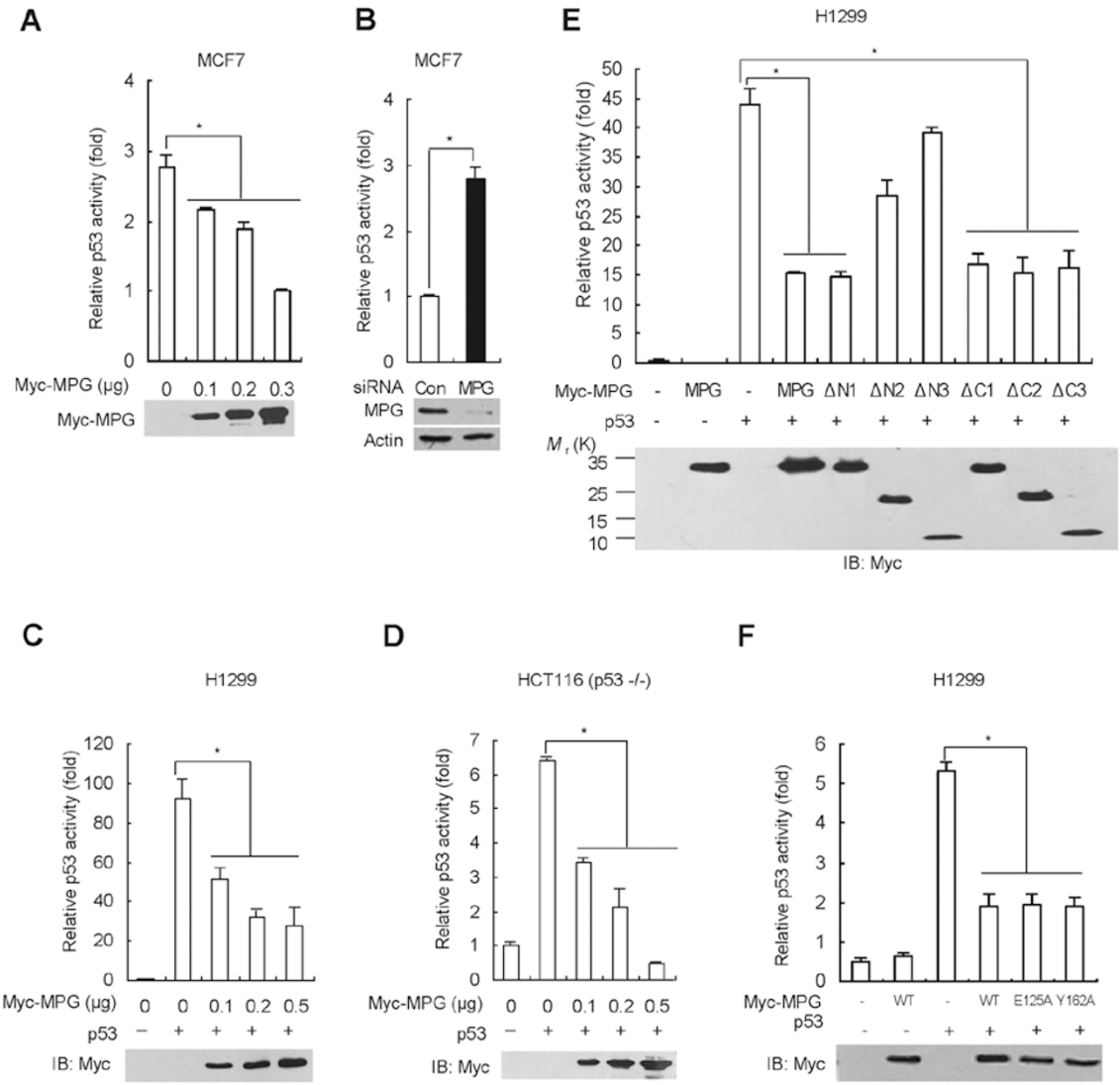

Figure 4 MPG represses p53-dependent transcriptional activity. **(A)** The activity of the pG13L reporter gene in p53 wild-type MCF7 cells transfected with increased MPG or a mock vector. Reporter activity was assayed as described in Materials and Methods and represents the mean ± SD of three separate experiments. *P < 0.05. **(B)** siRNA ablation of MPG increases the transcriptional activity of p53. MCF7 cells were transfected as indicated. After 48 h, the luciferase assay was performed. Data are mean ± SD. (n = 3). *P < 0.05. **(C**, **D)** The activity of the pG13L reporter gene in p53 null H1299 **(C)** or $p53^{-/-}$ HCT116 cells **(D)** co-transfected with p53 or a mock vector and increased MPG. The reporter activity was assayed and represented. Data are mean ± SD (n = 3). *P < 0.05. **(E)** The N-terminal region of MPG is required for inhibiting p53 transactivity. H1299 cells were co-transfected with p53 or the mock vector with deletion mutants of MPG. A luciferase assay was performed. Data are mean ± SD (n = 3). *P < 0.05. **(F)** MPG represses p53 activity independent of MPG glycosylase activity. H1299 cells were co-transfected with p53 or a mock vector with point mutations of MPG, as indicated. A luciferase assay was performed. Data are mean ± SD (n = 3). *P < 0.05.

a similar MPG binding affinity compared with wild-type p53 (MCF7) (Figure 3C), consistent with the exogenous Co-IP assay results (Figure 3B). Interestingly, the T256K, D259G and S260A mutations in Jurkat cells also attenuated the interaction with MPG (Figure 3C). These data indicate that certain residues within the p53 DBD (including R248, T256, D259, S260, R273 and R280) play critical roles in mediating the interaction with MPG, and some of the pathophysiologically occurring mutations in human tumors significantly weaken this interaction.

MPG represses p53-dependent transcriptional activity

Like other molecules in the DNA repair system, MPG cooperates with MBD1 for transcriptional repression [24]. To check whether MPG modulates the transcriptional activity of p53 by binding to p53, we expressed Myc-MPG with a luciferase reporter plasmid pG13L that contains 13 tandem repeats of the p53 responsive element in p53 wild-type MCF7 cells. MPG significantly inhibited the activity of endogenous p53 in a dose-dependent manner (Figure 4A). Knockdown of endogenous MPG by RNA interference (RNAi) significantly enhanced p53 activity in MCF7 cells (Figure 4B) and in HEK293 cells (Supplementary information, Figure S1B). To confirm the results, exogenous p53 was expressed in p53-null H1299 and HCT116 $p53^{-/-}$ cells together with pG13L and MPG. In the absence of exogenous p53, pG13L could not be activated; however, in the presence of exogenous p53, pG13L could be activated. The co-expression of MPG could inhibit p53 activity in a dose-dependent manner (Figure 4C and 4D). Given that the N-terminal aa 35-79 of MPG are required for p53 binding (Figure 2), we determined whether they are also important for the repressive activity. As shown in Figure 4E, a deletion of the p53-binding region in MPG removed the inhibitory effect of MPG on p53 activity, suggesting that their interaction is required for MPG to inhibit p53.

The MPG truncation that lacks residues 1-79 contains the same enzymatic activity and binding specificity as the full-length protein [19]. This implies that MPG represses p53 activity independently of the MPG glycosylase activity. To confirm this hypothesis, two point-mutation mutants of MPG, E125A and Y162A, were constructed. These two mutants have minimal glycosylase activity [25]. A p53-dependent reporter with wild-type MPG, E125A, Y162A and p53 were co-transfected into H1299 cells. Wild-type MPG, E125A and Y162A had the same ability to significantly repress the transcriptional activity of exogenous p53 (Figure 4F). These results support that MPG can efficiently repress p53 transcriptional activity independently of its enzymatic activity.

We also tested whether p53 had any effects on the glycosylase activity of MPG. Biotin-labeled hypoxanthine-containing oligos were incubated with purified MPG with or without p53 protein (Supplementary information, Data S1). As shown in Supplementary information, Figure S2, p53 had no significant effect on MPG excision activity.

MPG selectively inhibits p53 binding to pro-arrest target genes

To evaluate the effect of MPG on the transactivation function of p53, we first measured the DNA-binding activity of p53 to its downstream targets by electrophoresis mobility shift assays (EMSAs). We transfected a mock vector, MPG or p53 alone, or co-transfected p53 with different doses of MPG in H1299 cells and then harvested the nuclear extracts after 48 h. In the reaction buffer, Mg^{2+} was added to inhibit non-specific binding of MPG [26]. As shown in Figure 5A, MPG reduced the DNA-binding activity of p53 to its binding sites on p21, 14-3-3σ and Gadd45 to an almost undetectable level in a dose-dependent manner. Surprisingly, MPG had no significant effects on p53 binding to PUMA. For the controls, the vector and MPG alone produced no complexes with these oligonucleotides. These results suggest that MPG inhibits the DNA-binding ability of p53. Because the short probes of the examined p53 targets possess a highly conserved p53-binding consensus sequence, we propose that the preferential inhibition on the pro-arrest genes but not on pro-apoptotic PUMA by MPG might not be caused by the differences among the DNA sequences. Given that the protein used in the EMSA assays was isolated from the nuclear extracts of mammalian cells, MPG and its interacting proteins might play a role in the selection.

To further verify the differential effects of MPG on p53 binding to the targets, quantitative Chromatin immunoprecipitation (ChIP) assays by real-time PCR were carried out using control IgG or p53 antibody. Co-expression of MPG reduced occupancy of p53 at the promoters of p21, 14-3-3σ and the third intron of Gadd45, but it had no significant effect on the promoters of PUMA or PIG3 (Figure 5B). As a control, MPG itself could not be co-immunoprecipitated with these target genes. These data argue for a model in which MPG binds to p53 and selectively interferes with its binding to cell cycle arrest targets such as p21, 14-3-3σ and Gadd45.

MPG negatively regulates p53-mediated cell cycle arrest

We next examined the ability of MPG to regulate the transcription of p53 target genes. We measured the mRNA levels of typical target genes of p53 using quanti-

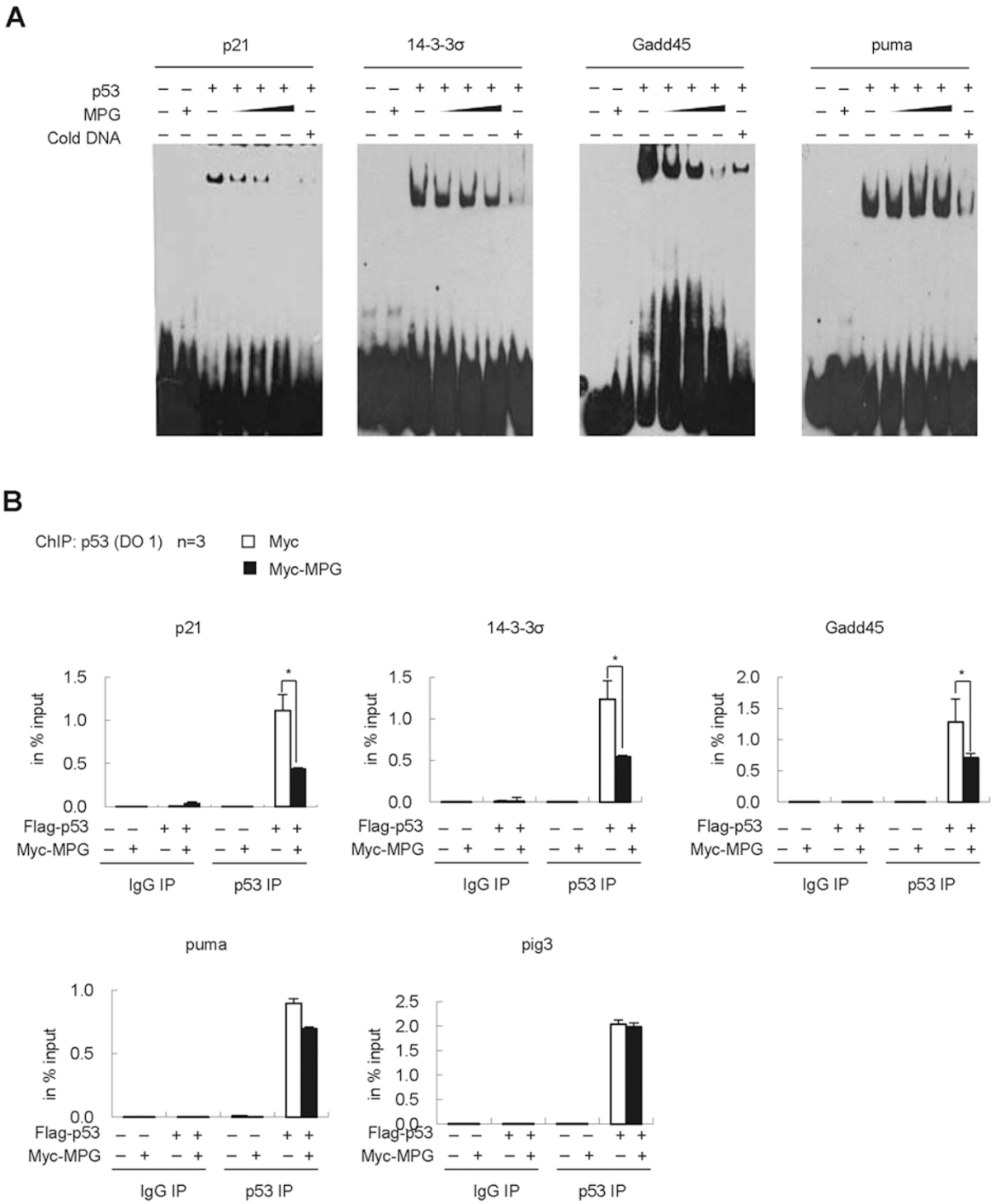

Figure 5 MPG preferentially inhibits the binding of p53 to the cell cycle arrest-related target genes. **(A)** *In vitro* EMSA assays. The DNA-binding activity of p53 to oligonucleotides containing the p53 binding sites of the p21 promoter, 14-3-3σ promoter, the third intron of Gadd45 or the PUMA promoter was determined. H1299 cells were transfected with p53 or MPG alone, or co-transfected with p53 and an increasing amount of MPG. After 24 h, the nuclear extracts were purified and used in the EMSA assays. **(B)** Multiple ChIP analysis on the consensus binding sequences of p53 targets. H1299 cells were transfected with a mock vector, MPG, p53, or co-transfected with p53 and MPG, as indicated. After 24 h, ChIP was carried out using a control mouse IgG or an anti-p53 antibody, and RT-PCR was performed for the indicated promoters. Data are mean ± SD (n = 3). *P < 0.05.

tative real-time RT-PCR in the presence of overexpressed MPG or knockdown of endogenous MPG in MCF7 cells. The overexpression of MPG significantly reduced the mRNA levels of pro-arrest genes, including p21, 14-3-3σ and Gadd45 but had only weak effects on the pro-apoptotic genes PUMA, Noxa and PIG3; the DNA repair gene p53R2; and the metabolism gene TIGAR (Figure 6A). Consistently, when MPG was knocked down, the mRNA levels of p21, 14-3-3σ and Gadd45 were increased; in contrast, PUMA, Noxa, PIG3, p53R2 and TIGAR showed little change (Figure 6B). Similar results were obtained in HEK293 cells (Supplementary information, Figure S3). The regulatory effect of MPG on the cell cycle arrest genes was dependent on p53, as in the p53-depleted MCF7 cells; MPG depletion had no significant effect on the expression levels of these genes (Figure 6C).

To confirm these results, we analyzed the expression of p53 target genes by western blotting. Overexpression of MPG downregulated the expression levels of p21, Gadd45 and 14-3-3σ, but not those of PUMA, Noxa, PIG3, TIGAR or p53 itself (Figure 6D). When MPG was depleted by RNAi, the protein levels of p21, Gadd45 and 14-3-3σ were upregulated, while those of PUMA, Noxa, PIG3, TIGAR and p53 remained unchanged (Figure 6E).

To examine whether MPG influences p53-mediated cellular effects, we measured cell cycle arrest and apoptosis. The knockdown of MPG induced a prominent G1 arrest in p53-proficient MCF7 cells but not in p53-depleted MCF7 cells (Figure 6F). In contrast, reducing the lower level of MPG had no significant effect on apoptosis (data not shown). Taken together, these data suggest that MPG negatively regulates p53-dependent cell cycle arrest but not apoptosis.

MPG releases p53 under alkylating agent-induced DNA damage

To explore how MPG balances the functions of glycosylase and p53 negative modulation in greater detail, we chose 3 different chemotherapeutic agents, 5-fluorouracil (5-FU), TMZ and MMS. 5-FU can block DNA synthesis while TMZ and MMS are known to induce genome-wide base damage, including 7-^{m}G and 3-^{m}A, which are the major substrates for MPG *in vivo* [27, 28]. Western blot analysis revealed that knockdown of MPG upregulated p21 and 14-3-3σ, but not p53, in MCF7 cells (Figure 7A, lanes 1 and 2). Following an exposure to 5-FU for 4 h, the effects of MPG depletion on p21 and 14-3-3σ were not changed (Figure 7A, lanes 3 and 4). By contrast, TMZ and MMS treatment induced p21 and 14-3-3σ expression, and MPG depletion had no further effects on the increase (Figure 7A, lanes 5-8), implying that MPG lost the ability to regulate p53 activity under TMZ and MMS treatment. Phosphorylation of p53 at Ser15 was used to verify the activating effect of each drug. Indeed, upon treatment with TMZ or MMS, but not 5-FU, the exogenous expression of MPG failed to inhibit the transcriptional activity of p53 in MCF7 cells (Figure 7B).

Because the MPG repression of p53 is dependent on their interaction, we then examined the endogenous interaction between p53 and MPG after DNA damage. Four hours after TMZ or MMS treatment, the interaction between MPG and p53 was significantly attenuated; treatment with 5-FU had no such effect (Figure 7C). The above results suggest that MPG had decreased ability to modulate p53 upon DNA damage induced specifically by alkylating agents.

MTS assay was used to measure cellular survival following MMS exposure. Cell survival measured by the MTS assay includes not only actively proliferating cells but also all metabolically active cells and is based on the assumption that dead cells do not reduce tetrazolium [29]. MCF7 cells were transfected with MPG or co-transfected with p53 or p53 mutant R248Q (which cannot bind to MPG with high affinity as shown in Figure 3) and MPG. MTS assays were carried out 24 h after MMS exposure. Results of > 10 independent experiments showed that MPG- but not p53-overexpressing cells were significantly more sensitive to the cytotoxic effects of MMS (Figure 7D). Co-expression of p53 with MPG reversed the effect of MPG, leading to enhanced cell survival. By contrast, the p53 mutant, which cannot efficiently bind to MPG had no such rescue effect (Figure 7D).

The fact that MPG lost its ability to negatively modulate p53 upon exposure to alkylating agents prompted us to speculate that MPG may be involved in tumorigenesis or be potentially beneficial in tumor therapy. We then examined the expression of MPG and p53 proteins in human cancer samples. Immunohistochemical staining of paired breast ductal carcinoma (BDC), lung squamous cell carcinoma (LSCC) and CC samples was performed (Figure 7E). Analysis of the stained tissue samples showed that the expression of MPG was positive in 38.7% of BDC, 43.4% of LSCC and 25.3% of CC cases and negative in all adjacent normal tissues. The percentages of the cases expressing a high MPG but low p53 (wild type) are 19.4% (BDC), 17.0% (LSCC) and 12% (CC) (Table 2). These results suggest a possible role of MPG overexpression in the development of human cancers. Collectively, the above findings provide new insights into the functional linkage between MPG and p53 in cancer therapy.

Functional relevance of MPG-p53 interaction in BER

To demonstrate the physiological relevance of MPG

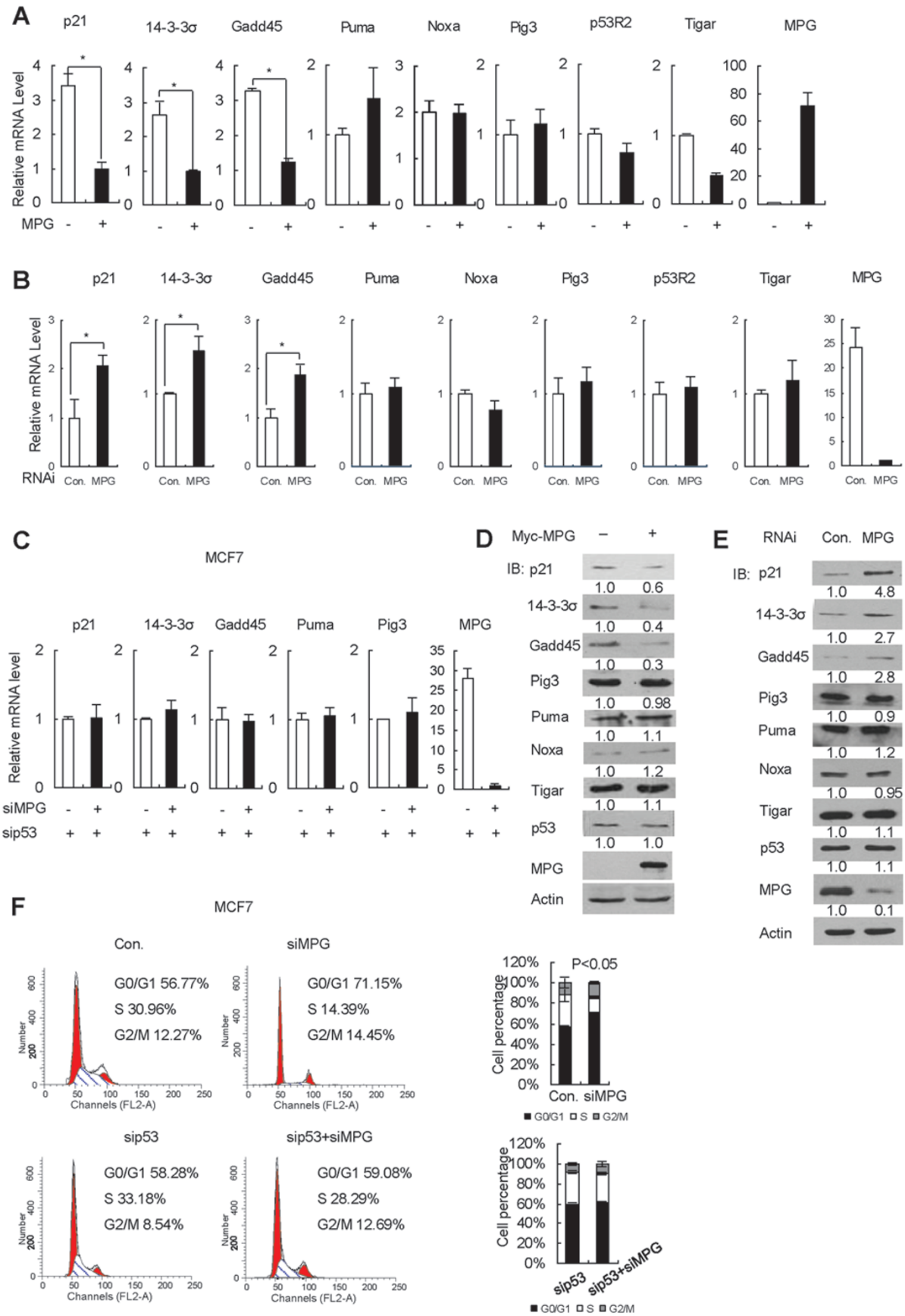
A
p21
14-3-3σ
Gadd45
Puma
Noxa
Pig3
p53R2
Tigar
MPG
Relative mRNA Level
MPG
B
RNAi
Con.
MPG
C
MCF7
Relative mRNA level
siMPG
sip53
D
Myc-MPG
IB: p21
14-3-3σ
Gadd45
Pig3
Puma
Noxa
Tigar
p53
MPG
Actin
E
RNAi
F
Con.
siMPG
sip53
sip53+siMPG
G0/G1 56.77%
S 30.96%
G2/M 12.27%
G0/G1 71.15%
S 14.39%
G2/M 14.45%
G0/G1 58.28%
S 33.18%
G2/M 8.54%
G0/G1 59.08%
S 28.29%
G2/M 12.69%
Number
Channels (FL2-A)
P<0.05
Cell percentage
G0/G1
S
G2/M

as a p53 negative modulator in regulating BER, MCF7 cells were transfected with MPG or co-transfected with p53 and MPG. After an exposure to MMS, the unrepaired intermediates of BER were assessed by the accumulation of DNA single-strand breaks (SSBs). We used an NAD(P)H depletion assay to measure the extent of SSBs [30, 31]. Accumulation of SSBs activates poly (ADP-ribose) polymerase 1 (PARP-1) that catalyzes the formation of polymers of poly(ADP-ribose), resulting in NAD^+ depletion. As seen in Figure 8A, SSBs were provoked after the cells were exposed to MMS, and the breaks were more produced when MPG, but not p53, was overexpressed. When MPG and p53 were co-expressed, the BER activity associated with SSB repair was restored only by wild-type p53 but not p53-R248Q mutant (Figure 8A). These results suggest that p53 activity on pro-arrest target genes and cell cycle arrest can modulate BER capacity.

To confirm these results, the single cell gel electrophoresis or comet assay was performed [29, 32, 33]. The alkaline comet indicates an increase of alkaline labile sites (AP sites or SSBs). Cells were assayed 4 h after treatment with MMS of different concentrations. Alkaline comet assay results showed significantly increased comet tails in the Myc-MPG group treated with MMS compared with vector control, indicating that cells produce AP sites and SSBs in response to MMS treatment, and that MPG overexpression resulted in more sensitivity to alkylating agent. When wild-type p53 and MPG were co-expressed, comet tails was shorter than MPG alone. By contrast, the p53-R248Q mutant had no such effect (Figure 8B and 8C).

As a support, the number of AP sites in MMS-treated cells was measured using the ARP assay [34, 35]. As predicted, more AP sites were detected in those cells where MPG was overexpressed alone than in the cells where MPG and wild-type p53 were co-expressed (Figure 8D). This is consistent with the suggestion that upon DNA alkylation stress, wild-type p53 dissociates from MPG and induces cell growth arrest. Then, AP sites are repaired efficiently, which leads to insensitivity to alkylating agents. By contrast, p53 mutants which have no transcriptional activity cannot induce cell cycle arrest and thus the AP sites are repaired with low efficacy.

Discussion

MPG is a critical glycosylase involved in the BER pathway to prevent alkylation-induced chromosome damage and cytotoxicity [36]. The N-terminal tail of MPG contributes little to MPG's recognition of substrates or N-glycosylase activity [19, 20, 37]. In the present study, we report that the N-terminal aa 34-79 of MPG plays a role in binding to p53 and inhibiting p53 activity. MPG regulates p53 transcriptional activity in a catalytic activity-independent manner. As far as we know, this is the first evidence to clearly show a glycosylase-independent function of MPG. Thus, we propose a model that the N-terminal part of MPG mediates its p53-regulating function while the rest of MPG executes the glycosylase activity, and both actions coordinate to control the genomic stability.

Mapping analysis revealed that the aa 236-290 region within the DBD of p53 was critical for its interaction with MPG. More than 90% of p53 native mutations in human tumors were detected in this domain. Interestingly, three out of four loss-of-function mutants (i.e., R248Q, R273C and R280K) dramatically reduced the ability to interact with MPG (Figure 3). Mutations of p53 result in loss of the normal tumor suppressor function (LOF) but gain-of-function (GOF) of oncogene at the same time [38]. Whether the mechanisms also involve

Figure 6 MPG selectively downregulates the expression of pro-arrest p53 target genes. **(A)** The overexpression of MPG selectively downregulates the expression of pro-arrest p53 target genes. MCF7 cells were transfected with Myc-MPG or a mock vector. Total RNA was subjected to real-time RT-PCR analysis. Expression levels of p21, 14-3-3σ, Gadd45, PUMA, noxa, PIG3, p53R2 and MPG RNAs were determined by the comparative threshold cycle method. The values shown are the mean ± SD (n = 3). *P < 0.05. **(B)** A knockdown of MPG selectively upregulates pro-arrest p53 target genes. MCF7 cells were transfected with MPG siRNA or a control siRNA. Total RNA was subjected to real-time RT-PCR analysis. Data are mean ± SD (n = 3). *P < 0.05. **(C)** MPG regulates cell cycle arrest genes dependent on the presence of p53. MCF7 cells were transfected with p53 siRNA in combination with a control siRNA or MPG siRNA. Total RNA was subjected to real-time RT-PCR analysis. Data are mean ± SD (n = 3). **(D)** Protein expression analysis of p53 target genes in the presence of overexpressed MPG. MCF7 cells were transfected with Myc-MPG. After 24 h, protein expression analysis was performed by western blotting with the indicated antibodies, as shown. Quantitative analysis was performed by measuring the integrated optical density. **(E)** Protein expression analysis of p53 target genes when MPG was depleted by RNAi. MCF7 cells were transfected with siRNA against MPG or a control siRNA. After 48 h, protein expression was analyzed by western blotting. **(F)** siRNA knockdown of MPG induces a p53-dependent cell cycle arrest. MCF7 cells were transfected with the MPG siRNA, p53 siRNA or MPG siRNA plus p53 siRNA as indicated. After 48 h, the cell cycle distribution characteristics were determined by flow cytometry. Data are mean ± SD (n = 3). *P < 0.05.

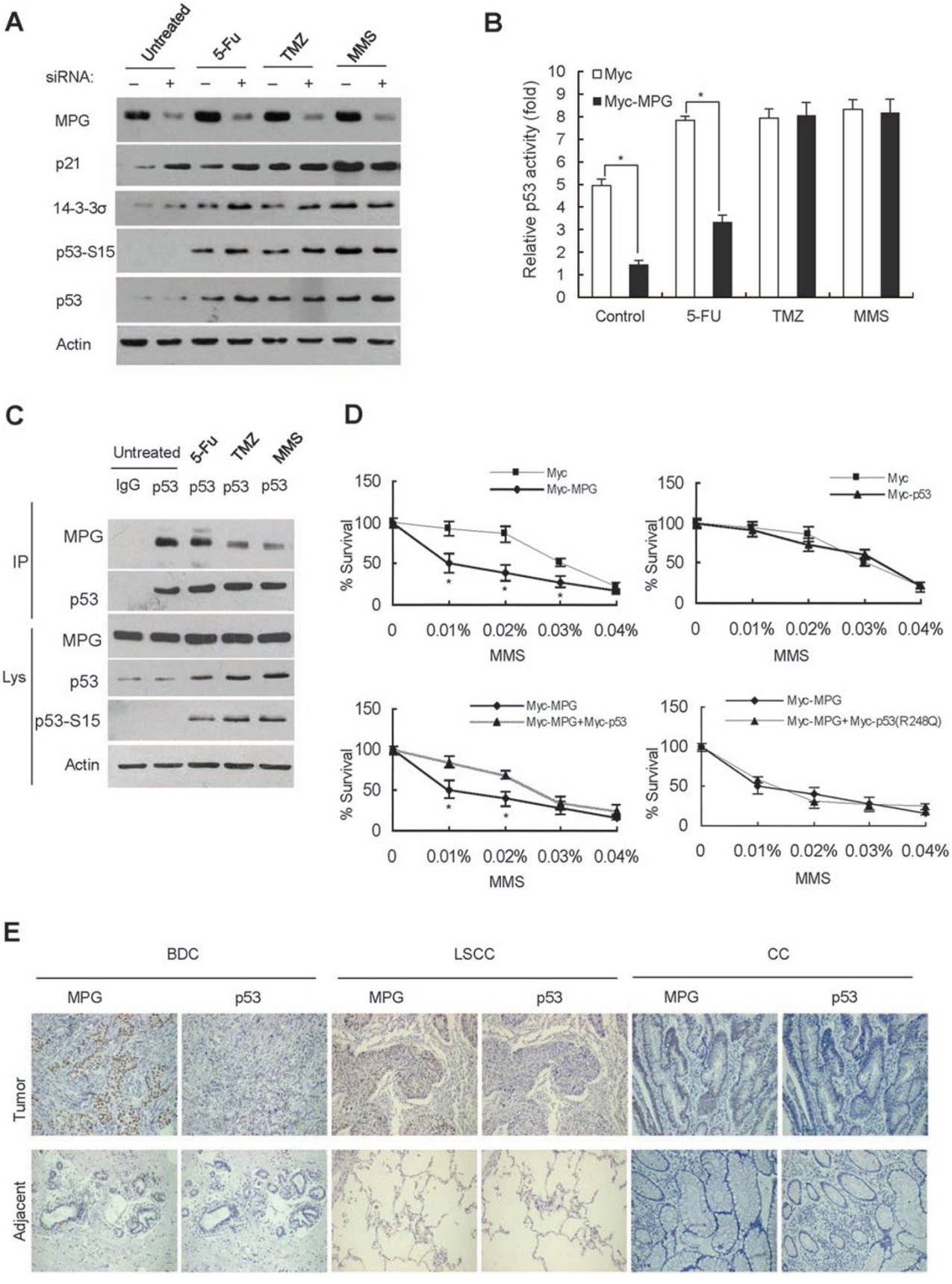
A
Untreated
5-Fu
TMZ
MMS
siRNA:
MPG
p21
14-3-3σ
p53-S15
p53
Actin
B
Myc
Myc-MPG
Relative p53 activity (fold)
Control
5-FU
TMZ
MMS
C
Untreated
5-Fu
TMZ
MMS
IgG
p53
IP
Lys
D
Myc
Myc-MPG
Myc-p53
Myc-MPG+Myc-p53
Myc-MPG+ Myc-p53(R248Q)
% Survival
MMS
E
BDC
LSCC
CC
Tumor
Adjacent

Table 2 MPG and p53 expression in human cancer tissues

	MPG positive and p53 negative	Both MPG and p53 positive	Both MPG and p53 negative	MPG negative and p53 positive	Total
Breast ductal carcinoma					
Adjacent	0	0	58.0%(18/31)	41.9%(13/31)	31
Tumor	19.4%(6/31)	19.4%(6/31)	16.1%(5/31)	48.4%(15/31)	31
Lung squanous cell carcinoma					
Adjacent	0	0	98.1%(52/53)	1.9%(1/53)	53
Tumor	17.0%(9/53)	26.4%(14/53)	11.3%(6/53)	45.3%(24/53)	53
Colon cancer					
Adjacent	0	0	98.7%(74/75)	1.3%(1/75)	75
Tumor	12%(9/75)	13.3%(10/75)	29.3%(22/75)	45.3%(34/75)	75

MPG is an important avenue for future studies.

The DBDis important for p53 to recognize the consensus sequence in target genes and transactivate the downstream genes to induce cell cycle arrest or apoptosis. Therefore, we measured the DNA-binding activity of p53 in the presence of MPG. In unstressed cells, the ability of exogenous p53 to bind to cell cycle control genes, such as p21, 14-3-3σ and Gadd45, was abolished by MPG in a dose-dependent manner. In contrast, there were no significant changes for pro-apoptotic genes. Moreover, the mRNA and protein levels of p21, 14-3-3σ and Gadd45 were regulated by MPG overexpression or knockdown and such regulation was dependent on the presence of p53. Indeed, in MCF7 cells that contain wild-type p53, reducing the level of MPG induced G1 arrest without a significant induction of apoptosis. Notably, MPG binds to p53 with a strong affinity as the endogenous interaction between MPG and p53 was easily detected by Co-IP assays. Therefore, we propose that MPG acts was a constitutive regulator of p53 in unstressed cells to control cell cycle arrest. In contrast to the functional mode of MPG, Hzf (another selective pro-arrest regulator of p53) is induced by p53 and then helps p53 to control the cell cycle arrest [8]. MPG expression seems to be independent of the p53 status and cannot be induced by p53 or DNA damage.

This prompts the following question: why does MPG preferentially regulate the pro-arrest p53 target genes over the pro-apoptotic genes? We speculate that there may be three mechanisms by which interacting proteins coordinate with p53 to modulate downstream outcomes: (1) by regulating p53 protein levels, as low levels of p53 tend to associate with growth-arrest genes while higher levels favor pro-apoptotic genes and trigger apoptosis; (2) proteins that are transcription factors themselves can bind to promoter sites adjacent to p53 response elements in addition to binding to the p53 protein to selectively induce specific response genes; and (3) proteins bind to p53 and directly influence the ability of p53 itself to bind preferentially to particular DNA target sequences. We observed that MPG and p53 cannot mutually modulate each other's protein levels. Moreover, MPG itself cannot bind

Figure 7 Overexpression of MPG in human cancers confers an insensitivity to alkylating agents in the presence of p53. **(A)** MCF7 cells were transfected with MPG siRNA or a control siRNA. After 48 h, cells were treated for 4 h with each of the indicated drugs at the following concentrations: 5-FU (50 μg/ml), TMZ (2.5 mM), and MMS (0.01%). Whole-cell extracts were analyzed by immunoblotting with anti-MPG, p53, p21, 14-3-3σ, p53/phospho-Ser15 and Actin antibodies. The expression of p53/phospho-Ser15 was used as an indicator of DNA damage. **(B)** MCF7 cells were co-transfected with pG13L and MPG or a mock vector. After 24 h, cells were treated with 5-FU, TMZ, or MMS for 4 h. The reporter activity for p53 was assayed. Data are mean ± SD (n = 3). *P < 0.05. **(C)** Co-IP of endogenous MPG and p53 from MCF7 cells in response to various DNA damage signals. The cells were treated with 5-FU, TMZ, or MMS for 4 h before harvest. Whole-cell lysates were immunoprecipitated with a p53 antibody (DO-1) or a control IgG. Both the lysates and the immunoprecipitates were analyzed by immunoblotting with the indicated antibodies. **(D)** MTS assay was used to determine cell survival. MCF7 cells were transfected with a mock vector, MPG or p53, or co-transfected with p53 and MPG or p53 mutant R248Q and MPG. After 24 h, cells were treated with the indicated concentration of MMS for 4 h. Points, average of at least three independent experiments. Data are mean ± SD (n = 3). *P < 0.05. **(E)** Representative immunohistochemical staining of MPG and p53 in human cancer tissues. Human BDC (left), LSCC (middle) and CC (right) are shown. Various cancer tissues and their normal-tissue counterparts (Adjacent) were analyzed simultaneously and all images were captured at 200× (Tumor, Adjacent).

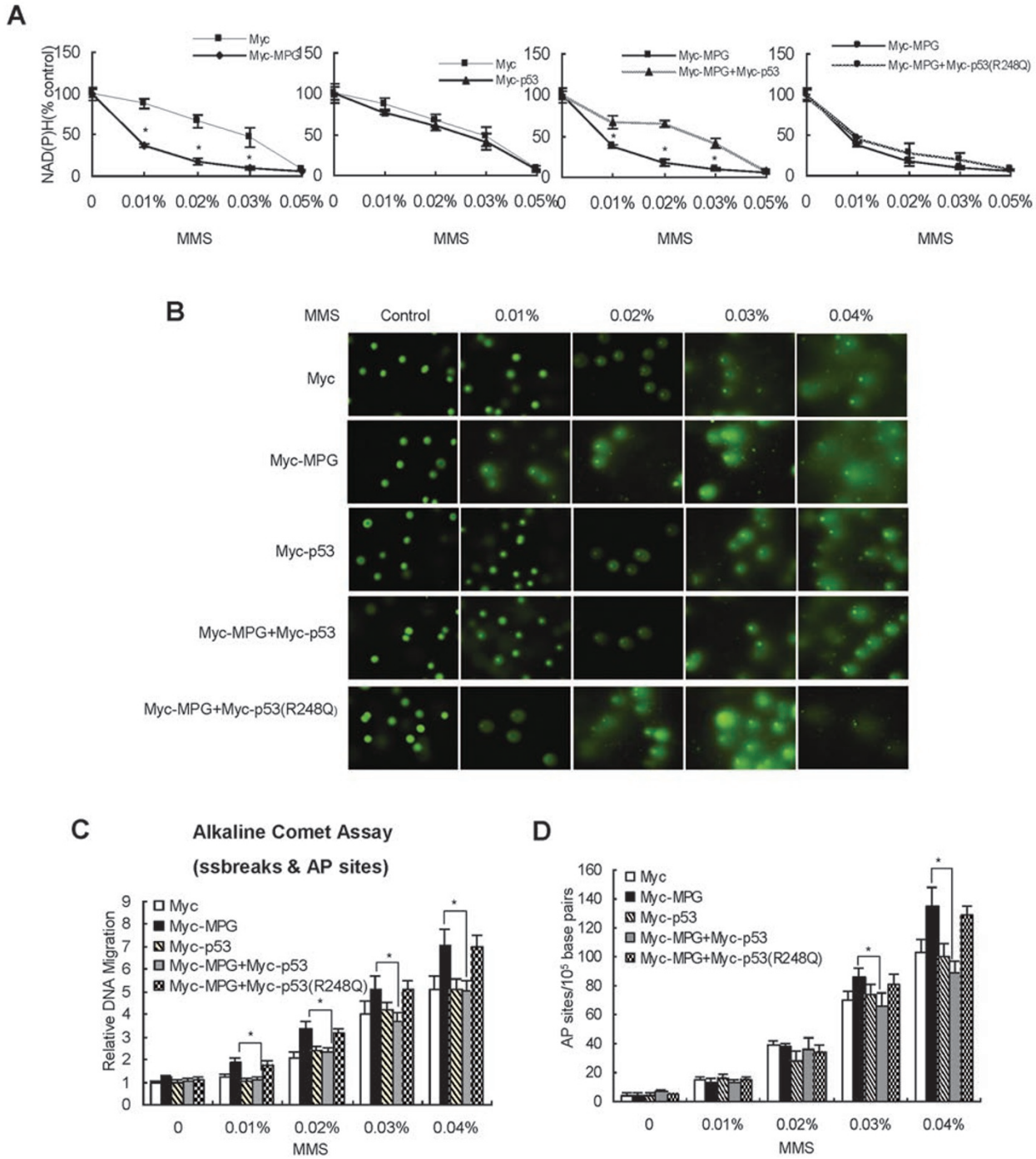

Figure 8 p53 activity on pro-arrest target genes and cell cycle arrest can modulate BER capacity. **(A)** Quantification of NAD(P)H depletion as an indicator of MMS-induced SSB accumulation. MCF7 cells were transfected with a mock vector, MPG or p53, or co-transfected with p53 and MPG or p53 mutant R248Q and MPG. After 24 h, cells were treated with the indicated concentration of MMS for 4 h. Data are mean ± SD (n = 3). *P < 0.05. **(B)** Representative alkaline comet assay images. MCF7 cells were transfected with a mock vector, MPG or p53, or co-transfected with p53 and MPG or p53 mutant R248Q and MPG. After 24 h, cells were treated with the indicated concentration of MMS for 4 h. **(C)** Alkaline comet analysis in **B** and quantified. Columns, average comet tail length of 100 individual cells. Data are mean ± SD (n = 100). *P < 0.05. **(D)** AP site determination in MCF7 cells after treatment with MMS. MCF7 cells were transfected with a mock vector, MPG, p53, or co-transfected with p53 and MPG or p53 mutant R248Q and MPG. After 24 h, cells were treated with the indicated concentration of MMS for 4 h. The assay was done in triplicate, three individual times. Data are mean ± SD (n = 3). *P < 0.05.

to p53 response elements directly. Our data strongly suggest that upon MPG binding to p53, p53 is preferentially inhibited from being recruited to the promoters of its cell cycle-arrest target genes, although the detailed selective mechanism is still unclear. We hypothesize that perhaps other unidentified co-factors in the complex with MPG help to confer the modulator function of MPG. We are currently exploring the components of the MPG complex using an immunoprecipitation assay combined with mass spectrometry analysis.

Cells are continuously exposed to damaging stimuli from normal cellular metabolism and environmental agents. BER is the major DNA repair pathway in mammalian cells for eliminating small DNA base lesions. The approximate 10^4 damaging events/mammalian cell that happen every day underscore the importance of BER. MPG can recognize and excise the damaged base resulting in a baseless or abasic or apurinic/apyrimidinic (AP) site. Unrepaired AP sites block DNA replication and transcription. Previous studies indicated that overexpression of MPG dramatically sensitized cells to alkylating agent-induced cytotoxicity by an increased production of AP sites (toxic repair intermediates) and strand breaks [12] and disrupted the normal BER. A recent study revealed that an inappropriate expression of human MPG can increase the accumulation of BER intermediates that promotes genomic instability [39]. MPG can specifically bind to DNA containing one and two base-pair loops within repetitive sequences, and the strength of this binding correlates with the extent of frameshift mutagenesis and microsatellite instability. In our study, we showed that increased MPG levels inhibit the ability of p53 to induce cell cycle arrest and shorten the DNA repair process, resulting in a reduction of BER and an accumulation of cytotoxic AP sites. It can be envisioned that MPG is kept at a low level in normal cells to avoid the accumulation of toxic repair intermediates and to maintain genomic stability. MPG overexpression may lead to a pronounced production of AP sites and an inhibition of cell cycle arrest induced by p53, both of which may contribute to overwhelming the downstream rate-limiting step of BER. The unbalanced repair may then contribute to genomic instability and tumorigenesis.

Another question is whether MPG plays a key role in reducing the p53-mediated cell cycle arrest in response to different types of genotoxic stress. An S phase-specific antimetabolite, 5-FU, interrupts thymidylate synthase and blocks the synthesis of the pyrimidine thymidine, which is a nucleotide required for DNA replication [40]. Cytotoxicity of MMS and TMZ caused by the alkylation of DNA is strongly attenuated by the ability of MPG to repair DNA lesions. When MPG is knocked down under such conditions, p21 and 14-3-3σ were not upregulated just after treatment with TMZ and MMS. Meanwhile, MPG lost the ability to bind and repress p53 transactivity (Figure 7). One possible explanation is that MPG dissociated from p53 and distributed widely over the genome to remove the damaged DNA caused by the alkylation agents. Interestingly, we observed that MPG overexpression occurs in breast ductal carcinoma, LSCC and CC samples (Figure 7); this is consistent with the low expression of p53 (which might be wild type due to the rapid dynamic degradation) in these cancer patients. Alkylating agents are clinically used in the treatment of several human cancers. The cytotoxicity of these anticancer drugs results from the alkylation of DNA and is strongly attenuated by the ability of the cells to repair DNA lesions. Besides being cytotoxic, these agents are also mutagenic and the occurrence of secondary cancers has been linked to the use of high-dose chemotherapeutic regimens. For those patients with high levels of MPG and wild-type p53, alkylating agents may increase the risk of secondary cancers or have diminished therapeutic effects. The pathophysiological relevance of MPG and p53 in cancers needs deeper investigation in the future.

In summary, this study shows that MPG, an important glycosylase in the BER pathway, specifically inhibits p53-mediated cell cycle arrest in a glycosylase-independent manner. The status of p53 coordinates with MPG to determine the sensitivity to alkylating drugs in cancer therapy. To the best of our knowledge, this is the first direct evidence to show that a DNA repair enzyme functions as a selective regulator of p53.

Materials and Methods

Plasmid constructs

Full-length, truncated, and point mutations of MPG and point mutations of p53 were constructed by inserting PCR amplified fragments into the related vectors. Detailed construct information of MPG was previously described [41]. A series of p53-truncated plasmids were gifts from Dr Shengcai Lin and described previously [41, 42]. Flag-p53 and Myc-p53 were a kind gift from Dr Yue Xiong, and pG13-Luc p53 luciferase construct was obtained from Dr Bert Vogelstein.

Cell culture and transfection

Human breast cancer MCF7 cells, BT474 cells, and MDA-MB-231 cells, human CC HCT116 cells (a kind gift from Dr Qimin Zhan) and human lung adenocarcinoma H1299 cells were cultured in DMEM medium (Hyclone) containing 10% fetal bovine serum (FBS; Hyclone). Human leukemia MOLT-4 cells and Jurkat cells were maintained in RPMI 1640 medium (Hyclone) with 10% FBS. Human CC HT29 cells were maintained in DMEM/F12 medium (Hyclone) containing 10% FBS. Cells were transfected with Lipofectamine 2000 following the manufacturer's

protocol (Invitrogen).

Antibodies and reagents

DNA-damage mimicking reagents 5-FU, TMZ and methylmethane sulfonate (MMS) were purchased from Sigma. Anti-Myc antibody was purchased from Clontech. Anti-FLAG and anti-Flag-HRP antibodies were from Sigma. Anti-MPG, anti-Myc-HRP, anti-p53 (DO-1), anti-p53-HRP, anti-p21, anti-pig3 and anti-Actin antibodies were from Santa Cruz. Phosphorylated p53 (Ser 15) and anti-puma antibodies were purchased from Cell Signaling. Anti-GST antibody was from Tiangen. Other antibodies used were anti-Gadd45 (Abnova), anti-14-3-3σ (NeoMarkers), anti-noxa (Bethyl Laboratories, Inc.) and anti-tigar (Abcam).

Immunoprecipitation and immunoblotting

Cells were harvested at 48 h post-transfection and lysed in HEPES lysis buffer (20 mM HEPES, pH 7.2, 50 mM NaCl, 0.5% Triton X-100, 1 mM NaF and 1 mM DTT) supplemented with protease inhibitor cocktail (Roche). Immunoprecipitations were performed using the indicated primary antibody and protein A/G-agarose beads (Santa Cruz) at 4 °C. Lysates and immunoprecipitates were examined using the indicated primary antibodies followed by detection with the related secondary antibody and the SuperSignal chemiluminescence kit (Pierce).

GST pull-down assay

Bacteria-expressed GST, GST-p53 or GST-MPG proteins were immobilized on glutathione-Sepharose 4B beads (GE, UK) and washed, and then beads were incubated with Myc-MPG or Myc-p53 expressed in H1299 cells and lysed in HEPES lysis buffer for 3 h at 4 °C under rotation. Beads were washed with GST binding buffer (100 mM NaCl, 50 mM NaF, 2 mM EDTA, 1% Nonidet P40 and protease inhibitor cocktail) and proteins were eluted, followed by western blotting.

RNA interference

The MPG siRNA (5′-AAGAAGCAGCGACCAGCTAGA-3′), p53 siRNA (5′-CUACUUCCUGAAAACAAC-3′) and non-targeting siRNAs (5′-UUCUCCGAACGUGUCACGU-3′) were synthesized by Shanghai GenePharm. All siRNAs were transfected into the cells according to the manufacturer's protocol. After 48 h, cells were washed with phosphate-buffered saline, lysed directly into sample buffer and resolved by 12% SDS-polyacrylamide gel electrophoresis.

Reporter gene assays

Luciferase reporter plasmids pG13-Luc (contains 13 tandem p53-binding elements) and pRL-CMV (internal control; from Promega) were co-transfected with plasmids indicated in figures . After transfection for 48 h, cells were lysed in 90 μl of a passive lysis buffer (Promega). Luciferase activity was measured with the Dual Luciferase Assay System (Promega) in accordance with the manufacturer's protocol.

Real-time RT-PCR

Real-time quantitative PCR was performed as described previously [5]. Sequences of primers of the p53 targeted genes used in qPCR assays are listed in Supplementary information, Table S1.

Fluorescence analysis

For detection of colocalization by immunofluorescence, cells were fixed with 4% paraformaldehyde and permeabilized in 0.2% Triton X-100 (PBS). Proteins were stained using the indicated antibodies and detected with a TRITC-conjugated or FITC-conjugated secondary antibody. The nuclei were stained with DAPI (Sigma), and images were visualized with a Zeiss LSM 510 Meta inverted confocal microscope.

Cell cycle analysis

Cells were transfected with MPG siRNA and non-targeting siRNAS as control. At 48 h post-transfection, cells were harvested by trypsinization, fixed in 70% ethanol and stained with propidium iodide (50 mg/ml) containing 1 mg/ml of RNase A at 37 °C for 30 min and then analyzed for DNA content.

Electrophoretic mobility shift assay

Forty-eight hours after transfection, cell nuclear extracts were made using a Nuclear Protein Extraction Kit (Fermantas). 10 μg of nuclear extract was incubated with biotin labeled oligonucleotides corresponding to p53 binding sites in p21 promoter, 14-3-3σ promoter, the third intron of Gadd45 and puma promoter in gel shift binding buffer (10% glycerol, 20 mM HEPES, pH 7.5, 25 mM KCl, 2 mM DTT, 2 mM $MgCl_2$, 0.2% NP40, 1 mg poly(dI-dC)). Unlabeled oligonucleotide was added in 200-fold excess as specific competitor. The DNA-protein complexes were then resolved by LightShift® Chemiluminescent EMSA Kit (Pierce) according to the manufacturer's instructions. The probe sequences of p53 targets are listed as follows. p21: GTCAGGAACATGTCCCAACATGTTGAGCTC; 14-3-3σ: GTAGCATTAGCCCAGACATGTCC; Gadd45: GTACAGAACATGTCTAAGCATGCTGGGGAC; puma: CGCGCCTGCAAGTCCTGACTTGTCCGCGGC.

Chromatin immunoprecipitation assay

H1299 cells were transfected with the expression plasmid for p53 together with or without the expression plasmid for MPG. Forty-eight hours after transfection, cells were treated with 1% formaldehyde at 37 °C for 15 min. After being washed with ice-cold PBS, cells were suspended with 200 ml of SDS lysis buffer (1% SDS, 10 mM EDTA and 50 mM Tris-HCl, pH 8.1) on ice for 10 min. Lysates were sonicated and insoluble materials were removed by centrifugation. Supernatants were then precleared with 80 μl protein-A beads for 1 h at 4 °C. The precleared chromatin solutions were immunoprecipitated with normal mouse IgG or with anti-p53 antibody at 4 °C overnight, followed by incubation with 60 ml of protein-A beads for 6 h at 4 °C. The beads were washed once with low salt wash buffer (50 mM HEPES pH 7.5, 140 mM NaCl, 1% Triton X100, 0.1% deoxycholate sodium, protease inhibitors), once with high salt wash buffer (50 mM HEPES pH 7.5, 500 mM NaCl, 1% Triton X100, 0.1% deoxycholate sodium, protease inhibitors), once with LiCl wash buffer (10 mM Tris pH 8.0, 250 mM LiCl, 0.5% NP-40, 0.5% deoxycholate sodium, 1 mM EDTA) and twice with 1 ml of TE buffer. Samples were eluted with 200 ml of the elution buffer (1% SDS and 0.1 M $NaHCO_3$) and then crosslinks were reversed by heating them at 65 °C for 6 h. Chromatin-associated proteins were digested with proteinase K at 45 °C for 1 h, and immunoprecipitated DNA was extracted with Phenol-chloroform followed by ethanol precipitation. Purified DNA was analysed by real-time PCR, using the SYBR Green mix

(Bio-Rad) with the MyIQ machine (Bio-Rad). Primers used for real-time PCR are available upon request.

Measurement of intracellular NAD(P)H

To quantification of intracellular NAD(P)H levels, MCF7 cells were seeded into 96-well plates and transfected with the indicated plasmids. After 24 h, they were treated with MMS (at the indicated concentrations) and CCK-8 solution (Dojindo Molecular Technology, Japan). The cells were then incubated for 4 h to allow formazan dye production, which was measured on a microplate spectrophotometer (SpectraMax 340PC384; Sunnyvale, CA) at 450 nm with 650 nm as the reference filter. The decrease in intracellular NAD(P)H levels were determined by comparing the absorbance of treated cells with that of the control. The means and standard errors for each cell line were calculated from at least three independent experiments, each in triplicate.

Immunohistochemical staining

The human multiple tissue arrays (MTA) of BDC (OD-CT-RpBre03-004), LSCC (OD-CT-RsLug04-004) and CC (OD-CT-DgCol01-006) were purchased from Shanghai Outdo Biotech (Shanghai, China). The clinical characteristics of all of samples could be downloaded from the company's Web site: http://www.superchip.com.cn/web/index.asp. Various cancer tissues and their normal tissues counterparts on MTAs were incubated simultaneously with MPG (4 μg/ml), p53 (2 μg/ml) antibodies or relative control IgG overnight at 4 °C. After washing with PBS, they were reacted with the biotin-labeled second antibody and then visualized using an ultrasensitive streptavidin-peroxidases system (Maxim Biotech, Fuzhou, China). The intensity of MPG and p53 for each individual case was quantified as described previously [43] and the percentage of expression were both graded as different scores. If the numerical value was higher or lower than that of the adjacent normal tissue, the expression of MPG and p53 in the tumor tissue was considered to be up-/down-regulated, respectively.

Cell survival assay

MCF7 cells were seeded into 96-well plates and transfected with the indicated plasmids. After 24 h, they were treated with MMS (at the indicated concentrations) 4 h, then drug-containing medium was removed and replaced with fresh growth medium. Cells were incubated for another 24 h, 0.05 mg/mL MTS reagent (Promega) was added to each well and incubated at 37 ºC for 4 h followed by absorbance measurement at 490 nm. The values were standardized to wells containing media alone.

Comet assay

The single-cell gel electrophoresis or comet assay was used to determine the extent of DNA damage in individual MCF7 cells, which transfected with the indicated plasmids treated with MMS. After 36 h, cells were treated with MMS for 4 h and harvested by trypsinization. Alkaline comet assay was done according to the manufacturer's instructions of OxiSelect™ Comet Assay Kit (Cell Biolabs, INC.). Comets were visualized by epifluorescence microscopy using a FITC filter [44]. The comet lengths of 100 individual cells per group were measured for each treatment group.

AP site determination assay

To determine number of AP sites formed, MCF7 cells were transfected with the indicated plasmids and treated with MMS. Cells were collected, and the genomic DNA was isolated using the Get-Pure DNA isolation kit (Dojindo Molecular Technologies, Rockville, MD). The ARP reagent specifically reacts with the aldehyde group of AP sites in the open conformation, converting them to biotin-tagged AP sites. The amount of biotin can then be quantified by an enzyme-linked immunosorbent assay-like assay [34]. The number of AP sites formed was determined using the AP Site Quantitation kit (Dojindo Molecular Technologies) as per the kit instructions [35]. The experiments were repeated in triplicate, and the data presented are averages of three independent experiments with standard error.

Statistical analysis

Statistical evaluation was carried out using a Student's *t*-test.

Acknowledgments

We thank Drs Shengcai Lin (Xiamen University), Bert Vogelstein (Johns Hopkins Oncology Center) and Yue Xiong (University of North Carolina) for providing materials. The study was supported by the National Basic Research Programs (2011CB910802, 2012CB910702, 2010CB912202), and National Natural Science Foundation Projects (31071144, 31125010).

References

1 Vousden KH, Lu X. Live or let die: the cell's response to p53. *Nat Rev Cancer* 2002; **2**:594-604.
2 Kern SE, Kinzler KW, Bruskin A, *et al*. Identification of p53 as a sequence-specific DNA-binding protein. *Science* 1991; **252**:1708-1711.
3 Harris SL, Levine AJ. The p53 pathway: positive and negative feedback loops. *Oncogene* 2005; **24**:2899-2908.
4 Dumaz N, Meek DW. Serine15 phosphorylation stimulates p53 transactivation but does not directly influence interaction with HDM2. *EMBO J* 1999; **18**:7002-7010.
5 Tian C, Xing G, Xie P, *et al*. KRAB-type zinc-finger protein Apak specifically regulates p53-dependent apoptosis. *Nat Cell Biol* 2009; **11**:580-591.
6 Sullivan A, Lu X. ASPP: a new family of oncogenes and tumour suppressor genes. *Br J Cancer* 2007; **96**:196-200.
7 Tanaka T, Ohkubo S, Tatsuno I, Prives C. hCAS/CSE1L associates with chromatin and regulates expression of select p53 target genes. *Cell* 2007; **130**:638-650.
8 Das S, Raj L, Zhao B, *et al*. Hzf Determines cell survival upon genotoxic stress by modulating p53 transactivation. *Cell* 2007; **130**:624-637.
9 Schnack C, Hengerer B, Gillardon F. Identification of novel substrates for Cdk5 and new targets for Cdk5 inhibitors using high-density protein microarrays. *Proteomics* 2008; **8**:1980-1986.
10 Samson L, Derfler B, Boosalis M, Call K. Cloning and characterization of a 3-methyladenine DNA glycosylase cDNA from human cells whose gene maps to chromosome 16. *Proc Natl Acad Sci USA* 1991; **88**:9127-9131.
11 Trivedi RN, Almeida KH, Fornsaglio JL, Schamus S, Sobol RW. The role of base excision repair in the sensitivity and resistance to temozolomide-mediated cell death. *Cancer Res*

2005; **65**:6394-6400.
12 Fishel ML, He Y, Smith ML, Kelley MR. Manipulation of base excision repair to sensitize ovarian cancer cells to alkylating agent temozolomide. *Clin Cancer Res* 2007; **13**:260-267.
13 Klapacz J, Lingaraju GM, Guo HH, *et al*. Frameshift mutagenesis and microsatellite instability induced by human alkyladenine DNA glycosylase. *Mol Cell* 2010; **37**:843-853.
14 Coquerelle T, Dosch J, Kaina B. Overexpression of N-methylpurine-DNA glycosylase in Chinese hamster ovary cells renders them more sensitive to the production of chromosomal aberrations by methylating agents--a case of imbalanced DNA repair. *Mutat Res* 1995; **336**:9-17.
15 Posnick LM, Samson LD. Imbalanced base excision repair increases spontaneous mutation and alkylation sensitivity in *Escherichia coli*. *J Bacteriol* 1999; **181**:6763-6771.
16 Gillen CD, Walmsley RS, Prior P, Andrews HA, Allan RN. Ulcerative colitis and Crohn's disease: a comparison of the colorectal cancer risk in extensive colitis. *Gut* 1994; **35**:1590-1592.
17 Hofseth LJ, Saito S, Hussain SP, *et al.* Nitric oxide-induced cellular stress and p53 activation in chronic inflammation. *Proc Natl Acad Sci USA* 2003; **100**:143-148.
18 Paik J, Duncan T, Lindahl T, Sedgwick B. Sensitization of human carcinoma cells to alkylating agents by small interfering RNA suppression of 3-alkyladenine-DNA glycosylase. *Cancer Res* 2005; **65**:10472-10477.
19 Lau AY, Scharer OD, Samson L, Verdine GL, Ellenberger T. Crystal structure of a human alkylbase-DNA repair enzyme complexed to DNA: mechanisms for nucleotide flipping and base excision. *Cell* 1998; **95**:249-258.
20 Lau AY, Wyatt MD, Glassner BJ, Samson LD, Ellenberger T. Molecular basis for discriminating between normal and damaged bases by the human alkyladenine glycosylase, AAG. *Proc Natl Acad Sci USA* 2000; **97**:13573-13578.
21 Berglind H, Pawitan Y, Kato S, Ishioka C, Soussi T. Analysis of p53 mutation status in human cancer cell lines: a paradigm for cell line cross-contamination. *Cancer Biol Ther* 2008; **7**:699-708.
22 Hollstein M, Sidransky D, Vogelstein, B, Harris CC. p53 mutations in human cancers. *Science* 1991; **253**:49-53.
23 Weisz L, Oren M, Rotter V. Transcription regulation by mutant p53. *Oncogene* 2007; **26**:2202-2211
24 Watanabe S, Ichimura T, Fujita N, *et al*. Methylated DNA-binding domain 1 and methylpurine-DNA glycosylase link transcriptional repression and DNA repair in chromatin. *Proc Natl Acad Sci USA* 2003; **100**:12859-12864.
25 Lee CY, Delaney JC, Kartalou M, *et al*. Recognition and processing of a new repertoire of DNA substrates by human 3-methyladenine DNA glycosylase (AAG). *Biochemistry* 2009; **48**:1850-1861.
26 Adhikari S, Toretsky JA, Yuan L, Roy R. Magnesium, essential for base excision repair enzymes, inhibits substrate binding of N-methylpurine-DNA glycosylase. *J Biol Chem* 2006; **281**:29525-29532.
27 Wood RD, Mitchell M, Sgouros J, Lindahl T. Human DNA repair genes. *Science* 2001; **291**:1284-1289.
28 Tentori L, Graziani G. Pharmacological strategies to increase the antitumor activity of methylating agents. *Curr Med Chem* 2002; **9**:1285-1301.
29 Rinne M, Caldwell D, Kelley MR. Transient adenoviral N-methylpurine DNA glycosylase overexpression imparts chemotherapeutic sensitivity to human breast cancer cells. *Mol Cancer Ther* 2004; **3**:955-967.
30 Chou WC, Wang HC, Wong FH, *et al*. Chk2-dependent phosphorylation of XRCC1 in the DNA damage response promotes base excision repair. *EMBO J* 2008; **27**:3140-3150.
31 Nakamura J, Asakura S, Hester SD, de Murcia G, Caldecott KW, Swenberg JA. Quantitation of intracellular NAD(P)H can monitor an imbalance of DNA single strand break repair in base excision repair deficient cells in real time. *Nucleic Acids Res* 2003; **31**:e104.
32 Swain U, Subba Rao K. Study of DNA damage via the comet assay and base excision repair activities in rat brain neurons and astrocytes during aging. *Mech Ageing Dev* 2011; **132**:374-381.
33 Olive PL, Banath JP. The comet assay: a method to measure DNA damage in individual cells. *Nat Protoc* 2006; **1**:23-29.
34 Kow YW, Dare A. Detection of abasic sites and oxidative DNA base damage using an ELISA-like assay. *Methods* 2000; **22**:164-169.
35 Bapat A, Glass LS, Luo M, *et al*. Novel small-molecule inhibitor of apurinic/apyrimidinic endonuclease 1 blocks proliferation and reduces viability of glioblastoma cells. *J Pharmacol Exp Ther* 2010; **334**:988-998.
36 Drablos F, Feyzi E, Aas PA, *et al*. Alkylation damage in DNA and RNA--repair mechanisms and medical significance. *DNA Repair (Amst)* 2004; **3**:1389-1407.
37 Labahn J, Scharer OD, Long A, *et al*. Structural basis for the excision repair of alkylation-damaged DNA. *Cell* 1996; **86**:321-329.
38 Dittmer D, Pati S, Zambetti G, *et al*. Gain of function mutations in p53. *Nat Genet* 1993; **4**:42-46.
39 Hofseth LJ, Khan MA, Ambrose M, *et al*. The adaptive imbalance in base excision–repair enzymes generates microsatellite instability in chronic inflammation. *J Clin Invest* 2003; **112**:1887-1894.
40 Longley DB, Harkin DP, Johnston PG. 5-fluorouracil: mechanisms of action and clinical strategies. *Nat Rev Cancer* 2003; **3**:330-338.
41 Miao F, Bouziane M, Dammann R, *et al*. 3-Methyladenine-DNA glycosylase (MPG protein) interacts with human RAD23 proteins. *J Biol Chem* 2000; **275**:28433-28438.
42 Rui Y, Xu Z, Lin S, *et al.* Axin stimulates p53 functions by activation of HIPK2 kinase through multimeric complex formation. *EMBO J* 2004; **23**:4583-4594.
43 Mi B, Wang X, Bai Y, *et al.* Beta-catenin expression is altered in dysplastic and nondysplastic aberrant crypt foci of human colon. *Appl Immunohistochem Mol Morphol* 2009; **17**:294-300.
44 Abner CW, Lau AY, Ellenberger T, Bloom LB Base excision and DNA binding activities of human alkyladenine DNA glycosylase are sensitive to the base paired with a lesion. *J Biol Chem* 2001; **276**:13379-13387.

(**Supplementary information** is linked to the online version of the paper on the *Cell Research* website.)